

Mn₂(CO)₁₀-VISIBLE LIGHT PHOTOMEDIATED, CONTROLLED RADICAL POLYMERIZATION OF MAIN CHAIN FLUORINATED MONOMERS AND SYNTHESIS OF BLOCK COPOLYMERS THEREOF

ALEXANDRU D. ASANDEI, OLUMIDE I. ADEBOLU, AND
CHRISTOPHER P. SIMPSON

University of Connecticut

2.1 INTRODUCTION

Fluoropolymers constitute a fundamental class of specialty materials endowed with wide morphological versatility, high thermal, chemical, aging, and weather resistance, as well as low surface energy, dielectric constant, flammability, refractive index, and moisture absorption. As such, their applications range from paints and coatings, pipe liners, transmission fluids, O-rings for extreme temperatures, fuel cell membranes, antifouling layers, etc., to optical fibers and high power capacitors [1]. Therefore, their precise synthesis is very relevant.

However, while controlled/living radical polymerizations (C/LRPs) have lately undergone remarkable developments [2–6], and atom transfer, nitroxide or addition–fragmentation methods [2] have proven quite successful for acrylates or styrenes,

their applicability in the CRP of *side-chain* fluorinated monomers such as pentafluoro styrene ($\text{CH}_2=\text{CH}(\text{C}_6\text{F}_5)$), fluorinated (meth)acrylates ($\text{CH}_2=\text{CHCOO}(\text{CH}_2)_n\text{R}_\text{F}$) or α -trifluoromethyl acrylates ($\text{CH}_2=\text{C}(\text{CF}_3)\text{COOR}_\text{alk}$) remains in its incipient stages [1]. Most importantly, their application in the CRP of the industrially significant, very reactive, gaseous, and thus experimentally difficult *main chain* fluorinated alkene monomers (FM), such as vinylidene fluoride (VDF, $\text{CH}_2=\text{CF}_2$), hexafluoropropene ($\text{CF}_2=\text{CF}(\text{CF}_3)$), tetrafluoroethylene ($\text{CF}_2=\text{CF}_2$), trifluorochloroethylene ($\text{CF}_2=\text{CFCl}$), still awaits demonstration.

Hence, due to the current lack of suitable CRP chemistry for these FMs and for the synthesis of well-defined complex architectures thereof (blocks, graft, hyperbranched, stars, etc.), the study and understanding of their self-assembly and of the properties and applications thereby derived, lag significantly behind those of the corresponding materials based on conventional monomers (styrene, acrylates, dienes, etc.). Thus, the development of FM-CRP and the synthesis of elaborate FM polymer designs is a worthy endeavor [7, 8]. Still, such polymerizations are very challenging on laboratory scale, as all FMs are gases ($b_\text{p}^{\text{VDF}} = -83^\circ\text{C}$) and typical telo/polymerizations are carried out at $T > 100\text{--}150^\circ\text{C}$ [1], in high pressure metal reactors. Moreover, in additional contrast with most monomers, the regioselectivity defects in VDF propagation leads to the formation of both $-\text{CF}_2-\text{CH}_2-\text{Y}$ and $-\text{CH}_2-\text{CF}_2-\text{Y}$ chain ends. Thus, regardless of the Y group of the reversible termination method in any potential LRP mechanism, the C–Y bond in $-\text{CF}_2-\text{CH}_2-\text{Y}$ will always be stronger than the one in $-\text{CH}_2-\text{CF}_2-\text{Y}$, thereby rendering the corresponding chain ends *dead*, not dormant, as far as reversible activation is concerned. Such chain ends will thus accumulate, broaden the PDI, and eventually lead to loss of control. Indeed, to the best of our knowledge there is no experimental evidence of the reversible activation of the “bad” chain ends in PVDF.

To date, the most successful approach to FM-CRP [1] remains the iodine degenerative transfer (IDT) [3, 9–14] ($\text{IDT: } \text{P}_n^\bullet + \text{P}_m\text{--I} \rightleftharpoons \text{P}_n\text{--I} + \text{P}_m^\bullet$) [1, 15, 16], an outcome of the earlier research on the high temperature ($100\text{--}230^\circ\text{C}$) free radical VDF telomerization [17, 18] with polyhalides [19], especially (per)fluorinated iodo chain transfer (CT) agents [16] such as $\text{CF}_3\text{--I}$ [20–23], $\text{CF}_3\text{--CF}_2\text{--I}$ [24], $\text{CF}_3\text{--}(\text{CF}_2)_3\text{--I}$ [25, 26], $\text{CF}_3\text{--}(\text{CF}_2)_5\text{--I}$ [21, 27–29], $(\text{CF}_3)_2\text{CF--I}$ [26], $\text{Cl--CF}_2\text{--CFCl--I}$ [23], $\text{I--}(\text{CF}_2)_{4-6}\text{--I}$ [10, 29, 30], but also with less active $\text{HCF}_2\text{CF}_2\text{CH}_2\text{--I}$ [27, 28], $\text{C}_6\text{F}_{13}\text{CH}_2\text{CF}_2\text{--I}$ [28, 31], and even CH_2I_2 [32], $\text{R}_\text{F}\text{--CH}_2\text{--CH}_2\text{--I}$ [33], or $\text{CH}_3\text{--I}$ [34]. In fact, IDT may be one of the oldest CRP methods, as a linear dependence of M_n on polymer yield was already demonstrated] in the early 1980s, and was the first industrial implemented CRP protocol [10–14].

In-depth modeling [30, 35] and kinetic [20, 27, 28] investigations have later revealed the importance of the structure and reactivity of the chain transfer agent (CTA) ($\text{I} > \text{Br} > \text{Cl} \sim \text{H}$ and difunctional better than monofunctional) [10, 16], as well as that of the contributions of side reactions (transfer to monomer and polymer, etc.) and monomer addition mode (1,2- vs. 2,1-) to the quality of the polymerization livingness. The synthesis of the iodo CTAs as well as some derivatization of the PVDF-I chain ends is available [16, 36].

However, VDF-IDT-CRPs always require a free radical source (*e.g.*, ^tbutyl peroxide (TBPO)), as *direct* metal catalyzed initiation from perfluoroiodides or any other halides is not available. This is a serious drawback with respect to the precise synthesis of block or graft copolymers based on FMs, as such systems would inevitably lead to mixtures of homo- and copolymers with the current technology. Therefore, the availability of an initiation method directly from halides, most likely mediated by transition metal catalysis, would be highly valuable.

Unfortunately, while VDF polymerization can proceed at ambient temperature [37], only very low VDF telomers (DP <1–3) may be obtained, and only at high temperature (>100°C) from transition metal salts and polyhalides by redox catalysis [1, 26, 38]. Moreover, while the 1:1 adduct formation by thermal or metal (Cu [39], Zn [40], Pd [41], SnCl₂/CH₃COOAg [42], Cp₂TiCl [43], PPh₃ [44], AIBN [45, 46], (NH₄)₂S₂O₈/HCOONa [47]) catalyzed addition of R_F-I derived perfluoroalkyl radicals to alkenes or of the R_F-Mt-I (Zn [48, 49], Zn/Cu [50]) organometallics to carbonyls and amides is available, the corresponding metal catalyzed addition of such electrophilic radicals to electrophilic fluorinated alkene substrates (FMs) at T <100°C, and especially at ambient temperatures is conspicuously absent from the literature. Thus, to the best of our knowledge, prior to our recent work [51, 52], there were no reports on metal-mediated FM or VDF polymerizations, let alone VDF-CRP. Consequently, the ability to carry out such reactions under mild conditions would be of great synthetic use, particularly in view of the great demand for perfluoroalkylation and trifluoromethylation reactions in organic chemistry [52] as well as in the initiation of the CRP of FMs and the synthesis of block, graft, and star FM copolymers.

Accordingly, and by contrast to styrene or acrylate CRPs which can be conveniently sampled from the side arm of a Schlenk tube on, for example, a 1 g scale, kinetic studies of VDF polymerizations involve many one-data-point experiments. This is very time-consuming and expensive due to the typical lab unavailability of a large number of costly metal reactors, which moreover still require hundreds of grams of monomer. Thus, development of methods that enable small-scale (1 g) polymerizations to proceed at room temperature (rt) in inexpensive, low pressure glass tubes would be highly desirable, as they could be adapted for fast screening of a wide range of catalysts and reaction conditions, and take advantage of photochemistry.

2.2 VDF PHOTOPOLYMERIZATION CATALYST SELECTION

Toward the above goal, in a large number of preliminary experiments we initially attempted the VDF polymerization at moderate temperatures (25–60°C) in low pressure glass tubes *via* conventional LRP methods (*e.g.*, Cu-ATRP [53], nitroxides, RAFT, Cp₂TiCl [54, 55]). However, all polymerizations were unsuccessful, most likely due to the inability of the particular systems to generate radicals reactive enough to add to VDF, or to reactivate the PVDF-Y chain ends at or around rt, or due to PVDF *vs.* catalyst solvent incompatibility [54]. Indeed, while, for example,

CuX/L abstracts halides from activated substrates (esters, benzyl, etc.), it hardly does so from perfluorohalides ($k_{(\text{CH}_3)_2\text{C}(\text{COOEt})-\text{Br}}/k_{\text{C}_8\text{F}_{17}-\text{Br}} > 10^2$) [56], and thus barely activates the C–I bond in $-\text{CF}_2-\text{CF}_2-\text{I}$, let alone in the “good” $-\text{CH}_2-\text{CF}_2-\text{I}$, and especially in the “bad” $-\text{CF}_2-\text{CH}_2-\text{I}$ PVDF chain end, and explains the failure of Cu-chemistry to provide PVDF-block copolymers. Moreover, activating amine Cu ligands are impractical with $\text{R}_\text{F}-\text{I}$ initiators due to the formation of ammonium salts or charge transfer complexes [57]. In addition, potential metal-mediated radical processes involving C–Mt bond formation will be plagued by $\beta\text{-H}$ and $\beta\text{-F}$ eliminations [54]. As such, as none of the conventional $\text{R}-\text{CF}_2-\text{I}$ activations or LRP protocols tested proved effective, we decided to investigate alternative means of radical generation and trapping [58, 59].

Interestingly, high power UV-photoinduced *telomerizations* are available for VDF [19, 60, 61]. Moreover, we have also shown [54, 62–65] that the free radical polymerization (FRP) of VDF occurs readily under UV irradiation at rt in the presence of TBPO. However, UV irradiation degrades most organometallic complexes, as well as RAFT reagents. To the best of our knowledge, prior to our work, there were [51, 52] no reports on the VDF polymerization using regular *visible* light. Thus, to maintain an ambient reaction temperature and a low pressure polymerization in the glass tubes, we decided to investigate photopolymerizations mediated by commercially available, low wattage (<30 W), spiral, compact, white light fluorescent bulbs.

Since VDF is a very reactive monomer, successful rt initiators should provide highly reactive, destabilized alkyl, semifluorinated, or perfluoroalkyl radicals. Thus, the visible light generated $\text{L}_\text{n}\text{Mt}^\bullet$ metal radical species should be a very good halide abstractor, and, for possible catalyzed CRP, $\text{L}_\text{n}\text{Mt}-\text{X}$ should also be a very good halide donor.

As such, similarly to the $\text{ClCp}_2\text{Ti}-\text{TiCp}_2\text{Cl}$ dimer chemistry we previously described for the CRP of styrene [66] and isoprene [67], but which was unsuccessful for VDF [54], prototypical examples [58, 59] of radically photolyzable transition metal complexes are based on dimers of the $(\text{CO})_n\text{Mt}-\text{Mt}(\text{CO})_n$ type. Out of many known examples, the following $\text{Re}(\text{CO})_5^\bullet > \text{Mn}(\text{CO})_5^\bullet > \text{CpW}(\text{CO})_3^\bullet > \text{CpMo}(\text{CO})_3^\bullet > \text{CpFe}(\text{CO})_2^\bullet > \text{Co}(\text{CO})_4^\bullet$ order is available in terms of their ability to abstract halides [68]. Although $\text{Re}(\text{CO})_5^\bullet$ ($\lambda_{\text{max}} = 535\text{--}550\text{ nm}$) abstracts Cl from CCl_4 ~65 times faster than $\text{Mn}(\text{CO})_5^\bullet$ [68, 69], the stronger Re–Re [70] bond dissociation energy (BDE) and its higher cost make the relatively inexpensive $\text{Mn}_2(\text{CO})_{10}$ [71] dimer [72] the most popular reagent in the series [59]. At rt, in the dark the dimer is stable, ($K_{\text{eq}} < 2.4 \times 10^{-19}$) [73], but as the Mn–Mn linkage is relatively weak (20–40 kcal/mol) [59, 74, 75], and further decreased by extra ligands [76], $\text{Mn}_2(\text{CO})_{10}$ undergoes both thermal ($\sim 90^\circ\text{C}$) [77] and facile rt photo homolysis. Indeed, while UV irradiation leads to CO loss, forming $\text{Mn}_2(\text{CO})_9$ and $\text{Mn}(\text{CO})_5^\bullet$, near-UV and visible longer wavelength ($\lambda = 366\text{--}400\text{ nm}$, $\lambda_{\text{max}}^{\text{Mn}_2(\text{CO})_{10}} = 324\text{ nm}$) provide the $\text{Mn}(\text{CO})_5^\bullet$ $17e^-$ paramagnetic metalloradical ($\lambda_{\text{max}}^{\text{Mn}(\text{CO})_5} = 780\text{--}830\text{ nm}$) [78] with good quantum efficiency [79, 80].

$\text{Mn}(\text{CO})_5^\bullet$ cleanly effects both hydride and halide abstraction from good RH donors such as Bu_3SnH [81], and respectively from RX halides with moderate BDEs (<310 kJ/mol) [82] such as CCl_4 [83], I_2 [83], polyhalides [82], allyl and benzyl

halides [82, 83], CH_3I [84], and other inactivated alkyl iodides, sometimes in the presence of InCl_3 [75, 82]. Phosphine ligands (PPh_3) depress the rates of such reactions [85]. Interestingly, and by contrast to other radical reagents, due to the CO ligand sterics, $\text{Mn}(\text{CO})_5^\bullet$ reacts faster with primary than secondary or tertiary halides [82]. Yet, while Mn-alkyls photolyze, they are not effective in radical reactions [75]. In addition, prior to our work [51–55], there were no examples of the use $\text{Mn}_2(\text{CO})_{10}$ for the radical activation of perfluoroalkyl halides, including trifluoromethylation reactions with $\text{CF}_3\text{--I}$ or $\text{CF}_3\text{--SO}_2\text{--I}$.

Interestingly, early reports proposed photo or thermal $\text{Mn}_2(\text{CO})_{10}$ or $\text{Re}_2(\text{CO})_{10}$ -mediated polymerizations initiated via either H abstraction from the monomer [86], addition of the metaloradical to tetrafluoroethylene to initiate its polymerization [87, 88], MMA [87, 89, 90] block copolymerization [91], or addition to 1,2-disubstituted acetyls and alkenes [92]. However, while preliminary polymerizations with $\text{Mn}_2(\text{CO})_{10}$ or $\text{Re}_2(\text{CO})_{10}$ and CCl_4 [93] or grafting from N-halogenated polyamides [94] were carried out in the 1960s, $\text{Mn}_2(\text{CO})_{10}$ was only recently employed in the thermal (60–90°C) [95] FRP of MMA or in the PMMA chain extensions from --CCl_3 groups on SiO_2 [96], chitosan [97], or from polystyrene-Br [98–100].

Very recently, $\text{Mn}_2(\text{CO})_{10}$ was, however, used as a photo-coinitiator for activated alkyl iodides (IDT) [101–103], or RAFT reagents [104] in controlled radical photo(co)polymerizations of VAc, acrylates, styrene, and alkenes, where $\text{Mn}(\text{CO})_5^\bullet$ irreversibly activated iodine terminated chains [101], but the *in situ* generated $\text{Mn}(\text{CO})_5\text{--I}$ [83] was not involved in the IDT.

Therefore, as $\text{Mn}_2(\text{CO})_{10}$ was never employed in polymerizations of main chain fluorinated monomers, or with inactivated alkyl halides or with perfluoroalkyl iodides, we decided to assess its scope and limitations as photo-coinitiator and to demonstrate that such $\text{L}_n\text{Mt--MtL}_n$ photolyzable transition metal complexes afford the initiation of VDF polymerization *directly* from a variety of regular and (per)fluorinated alkyl halides (Cl, Br, I) even at rt, thus opening up novel synthetic avenues for the photomediated synthesis of block and graft copolymers based on FMs. Second, we also set to kinetically explore such polymerization and investigate the possibility of $\text{Mn}_2(\text{CO})_{10}$ -mediated IDT–VDF–CRP. Third, we aimed to demonstrate the first examples of the synthesis of well-defined PVDF-block copolymers.

2.3 EFFECT OF REACTION PARAMETERS AND MECHANISTIC CONSIDERATIONS

2.3.1 Effect of Temperature and Light

While visible light could be invoked in the photodissociation of RX, control experiments revealed no polymerization in the dark, or with illumination, but in the absence of $\text{Mn}_2(\text{CO})_{10}$ [51]. Although polymerizations could easily be carried out anywhere from $T = 0^\circ\text{C}$ to $T = 100^\circ\text{C}$, we selected $T = 40^\circ\text{C}$ for all experiments, as a reasonable compromise between rate and a safe pressure inside the tube. In fact, simply

lowering the bottom part of the light bulb inside the oil bath helped maintain such temperature, with minimal additional heating from the hot plate [51].

2.3.2 Solvent Effect

Typical VDF laboratory polymerizations are carried out in acetonitrile (ACN) [18] that is a nonsolvent and a weak CTA. However, there is very little data [105–107] on the solvent effect in VDF polymerizations, let alone photopolymerizations. As such, as $\text{Mn}_2(\text{CO})_{10}$ is soluble in and inert toward most typical organic solvents (except for CCl_4 , CHCl_3), we decided to scan [51] a wide variety of polymerization media, noting that while good monomer/polymer solubilization and a photosensitizing solvent effect would be desirable, minimization of solvent CT outweighs solubility considerations. As such, the trends discussed below are the combined effect of the solvent CT transfer and polymer swelling ability, where the best solvents (alkyl carbonates) display minimum transfer and highest swelling. While we also carried out a similar study using Cp_2TiCl_2 , a solvent compatible with both $\text{Cp}_2\text{TiCl}^\bullet$ and PVDF could not be found [54].

Previous investigations of PVDF solution properties [108–113] have indicated that the best solvents are polar aprotic and H-bonding capable, and that HH sequences decrease solubility [108]. A common structural motif is a favorable H bonding interaction of the polar $\text{Y}=\text{O}$ bond ($\text{Y} = \text{C}, \text{S}, \text{P}$) of the solvent, with the mildly acidic Hs of $-\text{CF}_2-\text{CH}_2-\text{CF}_2-$. Accordingly, 2-pentanone, propionitrile, benzonitrile, nitrobenzene, $(\text{MeO})_3\text{P}$, $(\text{NEt}_2)\text{SO}_2$, sulfolane, and methylpyridines were classified as bad solvents. $(\text{BuO})_3\text{P}=\text{O}$ only swells PVDF, whereas γ -butyrolactone, propylenecarbonate, cyclohexanone, CH_3COPh , and $\text{Ph}_2\text{C}=\text{O}$ solutions gel on annealing at rt. Short chain phosphates $((\text{RO})_3\text{P}=\text{O}; \text{R} = \text{Me}, \text{Et}, \text{and } (\text{CH}_3)(\text{MeO})_2\text{P}=\text{O})$ are good solvents, while tertiary amides $(\text{HCONR}_2; \text{R} = \text{Me (DMF), Et, DMAc, N-formylmorpholine, NMP})$ and DMSO are very good solvents. Finally, cyclopentanone, N-alkyl cyclic urethanes as well as linear and cyclic ureas $((\text{Me}_2\text{N})_2\text{C}=\text{O}, [-\text{N}(\text{CH}_3)-(\text{CH}_2)_{2-3}-\text{N}(\text{CH}_3)-]\text{C}=\text{O}, \text{DMEU and DMPU})$ dissolve PVDF even at rt, with $[(\text{CH}_3)_2\text{N}]_3\text{P}=\text{O}$ (HMPA) and $(\text{CH}_3)[(\text{CH}_3)_2\text{N}]_2\text{P}=\text{O}$ considered excellent solvents.

The solvent effect in $\text{Mn}_2(\text{CO})_{10}$ polymerizations was explored with over 40 solvents [51] and perfluorobutyl iodide (PFBI), easily activated by $\text{Mn}(\text{CO})_5^\bullet$ (*vide infra*) was used as initiator. The comparisons were made under the same conditions ($\text{VDF/PFBI/Mn}_2(\text{CO})_{10} = 25/1/0.2$; $\text{VDF/solvent} = 1/3$ wt/v) and revealed that in accordance with the principles outlined above, no polymerization occurred in anisole, α, α, α -trifluorotoluene, diglyme, diethylene glycol monoethyl ether, ethyl ether, THF, dioxane, *o*-cresol, isopropanol, trifluoroacetic anhydride, tetramethylurea, sulfolane, benzonitrile, cyclopentanone even after 1–3 days. Poor reaction rates ($k_p^{\text{app}} < 1 - 9 \times 10^{-3} \text{ h}^{-1}$) were observed in HMPA, 2-butanone, methyl pentanone, DMF, DMSO, PEO, DMAc, δ -valerolactone, $^t\text{BuOH}$, and EtOAc. Slightly faster polymerizations ($k_p^{\text{app}} = 1 - 1.7 \times 10^{-2} \text{ h}^{-1}$) were seen in CH_2Cl_2 , acetic anhydride, γ -butyrolactone, 1,2-dichloroethane, TMP, MeOH, pentafluorobutane, and HFBz,

whereas β -butyrolactone, ϵ -caprolactone, ACN, and H_2O displayed medium rates ($k_p^{\text{app}} = 2.4 - 2.9 \times 10^{-2} \text{ h}^{-1}$).

While fast polymerizations occurred in diethyl-, di^tBu- and propylene carbonate ($k_p^{\text{app}} = 3 - 3.3 \times 10^{-2} \text{ h}^{-1}$), the fastest rates were provided by ethylene carbonate, HFIPA ($k_p^{\text{app}} = 5 - 7 \times 10^{-2} \text{ h}^{-1}$) and especially by dimethyl carbonate (DMC, $k_p^{\text{app}} = 1 \times 10^{-1} \text{ h}^{-1}$). The conversion, polymerization rate (k_p^{app}), M_n , and PDI were largely insensitive to the amount of DMC, ($V_{\text{tube}} = 35 \text{ mL}$, 1 g VDF, 1–12 mL DMC), whereas the rate significantly increased with the amount of VDF (*i.e.*, pressure and monomer concentration in solution, with 1–4 g VDF, 3–12 mL DMC). These are typical features of heterogeneous polymerizations of gaseous monomers [114], reminiscent of precipitation/dispersion polymerization of PVDF in scCO_2 with [29] and without [115] iodine CTAs. However, while fluorination enhances polymer solubilization, scCO_2 is a very poor PVDF solvent [116], even at high temperatures and pressures.

Thus, unfortunately, many of the good PVDF solvents (DMF, DMAc, ureas, etc.) act as strong CTAs and lead to no or very low conversions. However, remarkable trends are observed with carbonates, and especially with DMC, a green solvent [117]. Indeed, although DMC does not dissolve PVDF at rt, and similarly to ACN affords a heterogeneous polymerization, it provides by far the fastest reaction rates, at least thrice those obtained in ACN. Moreover, DMC consistently outperformed ACN not only for PFBI, but for all initiators tested including in polymerizations from poor initiators such as $\text{CF}_3-(\text{CF}_2)_2-\text{CO}-\text{Cl}$ or $\text{Cl}-\text{CF}_2-(\text{CF}_2)_6-\text{CF}_2-\text{Cl}$, which occurred *only* in DMC. Possible explanations for this trend include a photosensitizing effect or better monomer/polymer solubilization.

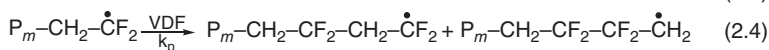
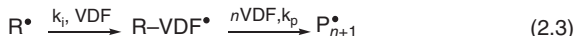
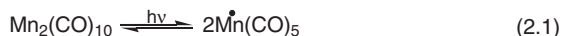
DMC is stable to pyrolysis and photolysis up to 350°C [118], but gas phase irradiation with high power Hg UV lamps induces some acetone promoted [119] decomposition at $T > 150\text{--}200^\circ\text{C}$ [120], while methyl and methoxy radicals form in the presence of nitric oxide [121]. Liquid phase DMC UV-photolysis with H_2O_2 [122], NO, NO_2 [123] or ^tbutylperoxide [124], additives occurs with H abstraction and formation of $\text{CH}_3-\text{O}-\text{CO}-\text{O}-\text{CH}_2^\bullet$, and solid state ^{60}Co γ -irradiation at 77°K produces methyl and methoxycarbonyl radicals [125, 126]. However, to the best of our knowledge, there are no reports on the photolysis or a potential photosensitizing effect of DMC under ambient visible light. Moreover, control experiments revealed that no photopolymerization occurs in DMC with VDF alone, VDF/ $\text{Mn}_2(\text{CO})_{10}$, or VDF/PFBI even after prolonged visible light exposure. Thus, while it may act as a weak CTA, DMC does not generate radicals under visible light. Accordingly, the better polymerization rates afforded by DMC are not a photo effect, but a consequence of its better VDF solubilization and PVDF swelling, which also enables better monomer diffusion to the propagating center. These results are consistent with studies on the solvent diffusion coefficient, and on PVDF swelling by carbonate solvents used as electrolytes for Li-ion batteries [127] containing PVDF microporous membranes [128–131], which revealed the same $\text{DMC} \gg \text{PC} \sim \text{EC} > \text{DEC}$ trend, a PVDF/DMC swelling ratio = 1.2 at 40°C, and possible dissolution of PVDF by DMC at high temperatures ($T > 80^\circ\text{C}$).

2.3.3 Polymerization Mechanism and Initiator Evaluation

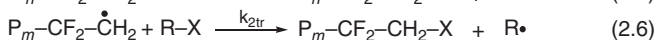
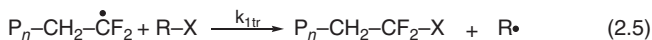
The proposed reaction mechanism is outlined in Scheme 2.1, with the setup previously described [51]. Initiation begins with the reversible photodissociation of $\text{Mn}_2(\text{CO})_{10}$ (Equation 2.1). Subsequent irreversible [101, 102] halide abstraction from R-X (and later PVDF-X), driven by the formation of high BDE Mn-X [74, 75, 132a], X = Cl, Br, I, (Equation 2.2) affords $\text{Mn}(\text{CO})_5\text{-X}$ and R^\bullet , which, if reactive enough, adds to VDF, thus initiating polymerization (Equation 2.3). As VDF is asymmetric, both 1,2- and 2,1-units, (Equation 2.4, head to tail HT, ~95% [20, 106] and respectively head to head, HH) occur in FRP (Equation 2.4). $\text{Mn}(\text{CO})_5^\bullet$ remains slowly but continuously photogenerated from the dimer throughout the polymerization, and, by abstracting X from R-X and PVDF-X (especially $\text{PVDF-CH}_2\text{-CF}_2\text{-I}$), maintains a steady state radical concentration by compensating for termination reactions.

2.3.3.1 Effect of Initiator Chain Transfer Constant on the Polymerization Mechanism If the amount of $\text{Mn}_2(\text{CO})_{10}$ is less than that of the initiator, depending on the value of its CT constant, ($\text{CT}_{\text{RX}}^{\text{PVDF}^\bullet} = k_{\text{transfer}}^{\text{PVDF}^\bullet \text{ to RX}} / k_{\text{propagation}}^{\text{VDF}}$), excess RX may act as a CTA vs. the propagating chains (Equations 2.5 and 2.6). Higher values ($\text{CT} > 1$) and X = I are required for controlled DT polymerizations [16], where such initiators are consumed very early in the process to provide iodide terminated polymeric CTAs

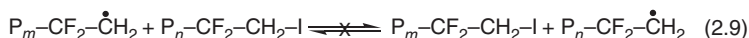
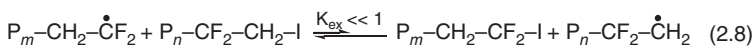
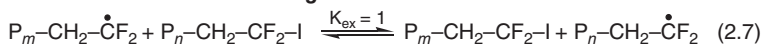
Initiation and Propagation



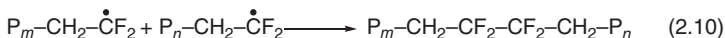
Chain Transfer to Initiator



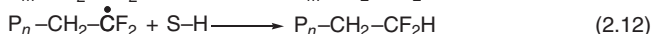
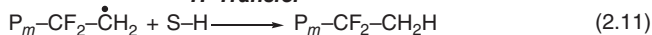
Iodine Degenerative Transfer



Bimolecular termination



H Transfer



SCHEME 2.1 Mechanism of $\text{Mn}_2(\text{CO})_{10}$ -mediated VDF-FRP and VDF-IDT-CRP.

[28, 51]. For PVDF, two such chain ends (*i.e.*, $P_n\text{--CH}_2\text{--CF}_2\text{--I}$ and $P_m\text{--CF}_2\text{--CH}_2\text{--I}$) are thus obtained [16, 27, 28, 31, 51].

Unfortunately, the $CT_{RX}^{PVDF^*}$ values of the initiators used herein or for related structures are only available in a few cases ($CT_{CCl_3Br} = 35$, $CT_{CCl_4} = 0.25$, $CT_{CHCl_3} = 0.06$ at 141°C [133], $CT_{C_6F_{13}\text{--I}} = 0.8$, $CT_{C_6F_{13}\text{--Br}} = 0.08$, $CT_{C_6F_{13}\text{--H}} = 0.0002$ in scCO_2 at 120°C [29]). Interestingly, perfluoroiodides and $\text{PVDF--CH}_2\text{--CF}_2\text{--I}$ have similarly large CT values ($CT_{C_6F_{13}\text{--I}} = 7.9$, $CT_{C_6F_{13}\text{--CH}_2\text{--CF}_2\text{--I}} = 7.4$), whereas the “bad” $\text{PVDF--CF}_2\text{--CH}_2\text{--I}$ 2,1-chain end is 25 times less active ($CT_{HCF_2CF_2CH_2\text{--I}} = 0.3$ at 75°C) [28]. Thus, the $\text{PVDF--CF}_2\text{--CH}_2^*$ propagating chain is correspondingly more reactive than $\text{PVDF--CH}_2\text{--CF}_2^*$. Obviously, the above CT data are apparent values, mol fraction-averaged over the two unequal reactivity growing chains, where clearly, $CT_{RX}^{VDF\text{--CH}_2^*} > CT_{RX}^{VDF\text{--CF}_2^*}$.

The possibility of initiation via H abstraction [81] was first tested from the $\text{--CF}_2\text{--H}$ group of 1H,1H,7H-dodecaheptafluoro acrylate, the C–H group of $(\text{CF}_3)_2\text{CH--OH}$, as well as from $\text{PVDF--CH}_2\text{--CF}_2\text{--H}$ chain ends, but no polymer was obtained, indicating that although such protons are more acidic, they are not abstracted by $\text{Mn}(\text{CO})_5^*$ at rt. A wide variety of over 40 halide structures never previously reported in conjunction with $\text{Mn}_2(\text{CO})_{10}$ (except for $\text{CH}_3\text{--I}$ [134], CCl_4 , RCCl_3 [93, 97], $(\text{CH}_3)_2\text{C}(\text{COOEt})\text{Br}$ [101, 102]), were subsequently evaluated [51].

However, no initiation was observed [51] from I_2 , tBu--I , $\text{CH}_3\text{--SO}_2\text{Cl}$, $\text{CH}_3\text{O--Ph--SO}_2\text{Cl}$, CH_2Cl_2 , CH_2I_2 , $\text{CHCl}_2\text{--CHCl}_2$, CHBr_3 , CHI_3 , CBr_4 , $\text{CH}_2=\text{CH--CH}_2\text{--Cl/Br/I}$, $\text{Ph--CH}_2\text{--Cl/Br/I}$, $\text{Ph--CH}(\text{CH}_3)\text{--Br}$, $\text{Ph}(\text{CH}_2\text{--Br/I})_2$, $\text{CH}_3\text{--CH}(\text{CN})\text{--Br}$, $\text{CH}_2(\text{CN})\text{--I}$, $(\text{CH}_3)_2\text{C}(\text{COOEt})\text{--Br/I}$, I--Ph--O--CH_3 , and NBS under a wide variety of conditions. As $\text{Mn}(\text{CO})_5^*$ has a very high halide affinity [59], abstraction is available in all cases. Therefore, the lack of initiation results from the corresponding radicals being more stable than the propagating PVDF^* radical, and thus failing to add at moderate temperatures, and being consumed by recombination or transfer.

By contrast, very reactive alkyl, polyhalide, as well as semi- and perfluorinated halide analogs of the above initiators such as CHCl_3 , CCl_4 , $\text{CCl}_3\text{--CCl}_3$, $\text{CF}_3(\text{CF}_2)_2\text{CO--Cl}$, $\text{CF}_3\text{--SO}_2\text{--Cl}$, $\text{Cl--CF}_2\text{--CClF--Cl}$, $\text{Cl--}(\text{CF}_2)_8\text{--Cl}$, $\text{--}(\text{CF}_2\text{--CFCl})_n\text{--}$, $\text{CCl}_3\text{--Br}$, $\text{EtOOC--CF}_2\text{--Br}$, $\text{Br--}(\text{CH}_2)_{10}\text{--Br}$, $\text{Br--CF}_2\text{--CH}_2\text{--CF}_2\text{--Br}$, $\text{Br--}(\text{CF}_2)_4\text{--Br}$, $\text{CH}_3\text{--I}$, $\text{CH}_3(\text{CH}_2)_5\text{--I}$, $\text{I--}(\text{CH}_2)_{10}\text{--I}$, $\text{C}_6\text{F}_5\text{--CF}_2\text{--I}$, $\text{H--CF}_2\text{--CF}_2\text{--CH}_2\text{--I}$, $\text{EtOOC--CF}_2\text{--I}$, $\text{Cl--CF}_2\text{--CFCl--I}$, $\text{CF}_3\text{--I}$, $\text{CF}_3\text{CF}_2\text{--I}$, $(\text{CF}_3)_2\text{CF--I}$, $(\text{CF}_3)_3\text{C--I}$, $\text{CF}_3(\text{CF}_2)_3\text{--I}$, and $\text{I--}(\text{CF}_2)_{4,6}\text{--I}$, all led to polymer formation [51]. The NMR demonstration of these initiations is outlined in Figure 2.1.

Remarkably, for VDF as well as for $\text{CF}_2=\text{CFCl}$, $\text{CF}_2=\text{CCl}_2$, $\text{CF}_2=\text{CFBr}$, $\text{CH}_2=\text{CFH}$, and for VDF random copolymers with $\text{CF}_2=\text{CF}(\text{CF}_3)$ and $\text{CF}_2=\text{CF}(\text{OCF}_3)$ [51], initiation occurred not only from polyhalides and all $\text{R}_F\text{--I}$ structures (which also provide IDT and elimination of HH defects), but even from semifluorinated models of the bad PVDF chain end ($\text{H--CF}_2\text{--CF}_2\text{--CH}_2\text{--I}$), and especially from simple inactivated alkyl iodides ($\text{CH}_3\text{--I}$). This indicates the feasibility of $\text{Mn}_2(\text{CO})_{10}$ -mediated block or graft VDF copolymerization *directly* from the halides above or their congeners regardless of their DT capability, when anchored on polymeric chains, surfaces, etc.

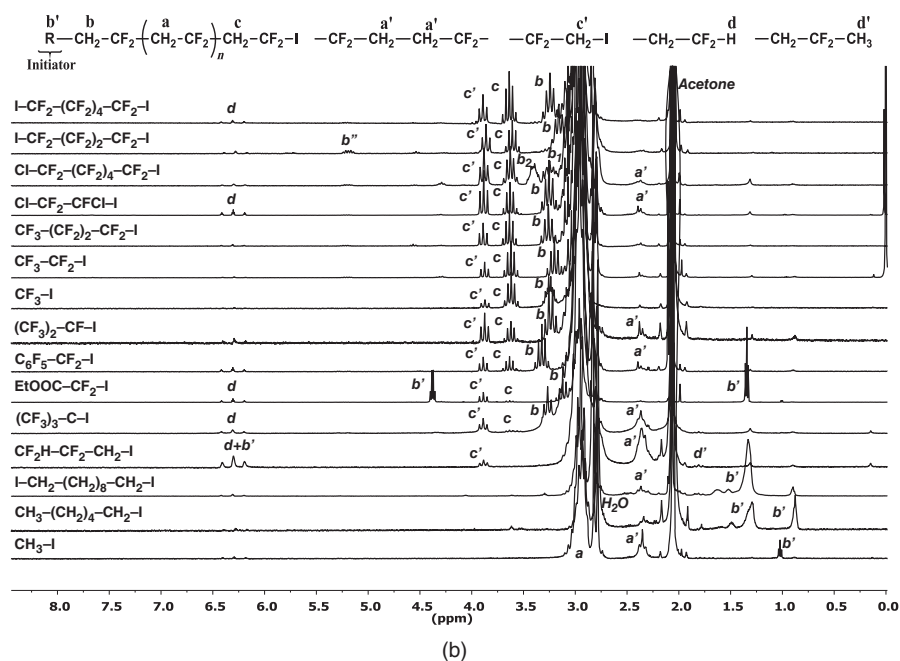
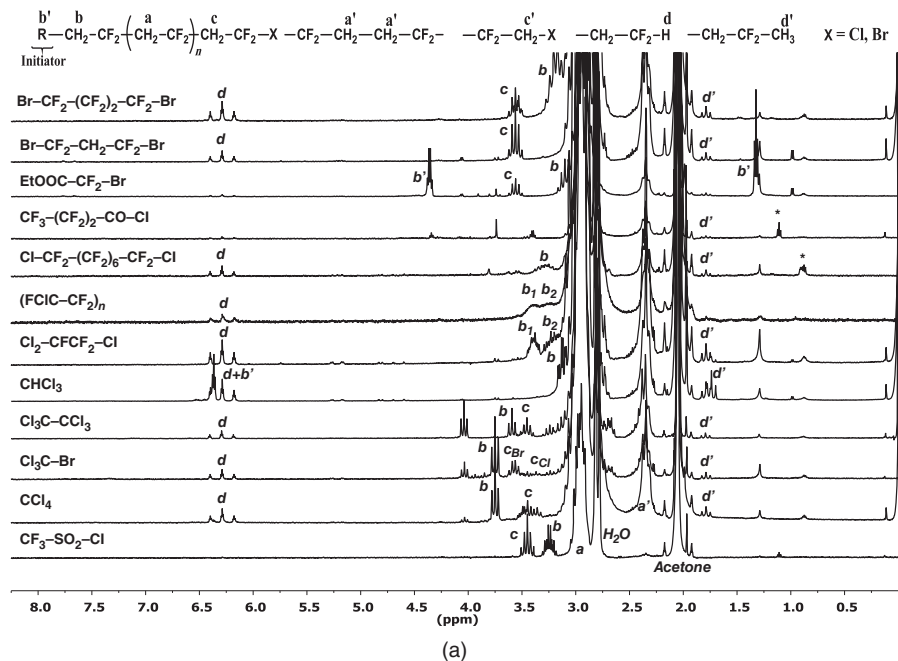


FIGURE 2.1 (a) ^1H -NMR spectra of $\text{Mn}_2(\text{CO})_{10}$ -photoinitiated PVDF from Cl and Br substrates. (b) ^1H -NMR spectra of $\text{Mn}_2(\text{CO})_{10}$ -photoinitiated PVDF from iodine substrates. Reprinted with permission from Reference 51. Copyright 2012 American Chemical Society.

Subsequent to initiation, the polymerization outcome is controlled by the combined effect of the relative order of $CT_{RX}^{PVDF^*}$ values (*i.e.*, C–X BDE in RX) [18, 29] (Equations 2.5 and 2.6)), the reactivity of fluorinated radicals (*i.e.*, more branched, more electrophilic) [135], and the preferential activation of primary *vs.* secondary or tertiary halides [82] by $Mn(CO)_5^*$. Accordingly, the initiators fall into three classes which require different amounts of $Mn_2(CO)_{10}$ for activation, and VDF undergoes FRP for R–X (X = Cl, Br, I) and IDT–CRP for R_F –I. These distinctions can easily be followed by inspecting the features of the halide chain ends in the corresponding PVDF NMRs (Figure 2.1).

First are the R–X species that provide only initiation and no chain transfer. Thus, initiators with strong R–X bonds (R–I, $CHCl_3$, and R_F –Cl, *i.e.*, Cl–CFCI– CF_2 –Cl, Cl–(CF_2 –CFCI) $_3$ –Cl, $CHCl_3$, CF_3 –(CF_2) $_2$ –CO–Cl, Cl– CF_2 –(CF_2) $_6$ – CF_2 –Cl, CH_3 –I, CH_3 –(CH_2) $_4$ – CH_2 –I, and I– CH_2 –(CH_2) $_8$ – CH_2 –I), do not undergo noticeable CT with PVDF*, demand stoichiometric $Mn_2(CO)_{10}$ activation and afford PVDF with no halide chain ends, and where the HH propagation is clearly noticed. The lack of polymer halide termini, stemming from the very low initiator CT value ($CT_{R-X} \ll 1$) and the larger amount of $Mn_2(CO)_{10}$ required, leads to VDF–FRP. Indeed, only $Mn(CO)_5^*$, and not the propagating chain can abstract the halide from RX.

In the second group, substrates with weak R–X bonds (CF_3SO_2 –Cl, R– CCl_3 , R_F –X, X = Br, I; *i.e.*, CF_3 – SO_2 –Cl, CCl_4 , CCl_3Br , CCl_3 – CCl_3 , Br– CF_2 – CH_2 – CF_2 –Br, Br– CF_2 – CF_2 – CF_2 –Br, EtOOC– CF_2 –Br), do undergo CT (Equations 2.5 and 2.6), require reduced (10%) amounts of $Mn_2(CO)_{10}$, and thus, at least one or both halide functionalized PVDF–X chain ends ($–CH_2$ – CF_2 –X and $–CF_2$ – CH_2 –X, X = Cl, Br, I, Figure 2.1) are observed. Moreover, if CT_{RX} is high (*e.g.*, CF_3 – SO_2 –Cl), HH defects may even be apparently suppressed. Here, the initiator is an efficient CTA, but the resulting PVDF halide chain ends are less reactive ($CT_{RX} > 1 > CT_{PVDF-CF_2-X} \gg CT_{PVDF-CH_2-X}$). Thus, as the Cl– and Br–DT exchange is inexistent, only VDF–FRP may ensue. Since none of the chain ends are reversibly activated, there will be no accumulation of PVDF– CH_2 –X, as both chain ends will abstract the halide from the initiator to provide the typical ~10/1 ratio of “good”/“bad” chain ends, similar to HT *vs.* HH propagation, unless the CT_{R-X} is so low, that only the more reactive PVDF– CH_2^* can abstract. Moreover, as $Mn(CO)_5^*$ could activate PVDF–X chains (X = Cl, Br) throughout the polymerization, a molecular weight increase may occur, albeit in a poorly controlled manner.

Finally, the best initiators for controlled VDF–IDT photopolymerizations and for high functionality PVDF–I for subsequent chain end derivatization or block copolymer synthesis are based on the semi and perfluorinated initiators. Thus, while good Cl and Br CTAs can at best provide efficient telomerizations [18], uncatalyzed halide DT–CRP occurs only for iodine [15–19].

Here, while poorer results are initially observed with H– CF_2 – CF_2 – CH_2 –I or $(CF_3)_3C$ –I where due to sluggish IDT ($CT_{RI} \sim CT_{PVDF-CH_2-I} < 1$), and respectively $Mn(CO)_5^*$ *vs.* R_F –I sterics issues, the PVDF– CH_2 –I chain ends and the HH units are still present, activated perfluoroalkyliodides such as CF_3 – CF_2 –I \sim $(CF_3)_2CF$ –I

$< \text{C}_6\text{F}_5\text{—CF}_2\text{—I}$, $\text{EtOOC—CF}_2\text{—I} < \text{Cl—CF}_2\text{—CFCl—I} < \text{CF}_3\text{—(CF}_2)_2\text{—CF}_2\text{—I} < \text{CF}_3\text{—I}$, $< \text{I—(CF}_2)_{4,6}\text{—I}$ provide not only *both* types of iodine chain ends but also suppression of HH propagation defects, and of termination by H transfer ($\text{—CF}_2\text{—H}$ and $\text{—CH}_2\text{—H}$), to below 1%. Most likely, their $\text{CT}_{\text{RF—I}}$ is comparable or better than that of $\text{C}_6\text{F}_{13}\text{—I}$ ($\text{CT}_{\text{C}_6\text{F}_{13}\text{—I}} = 7.9$) [28], thus enabling very efficient competition with both propagation and termination. As such, these high $\text{CT}_{\text{RF—I}}$ initiators suitable for IDT–CRPs [16] are converted early in the process into macromolecular PVDF–I CTAs [28], where the terminal $\text{P}_m\text{—CF}_2\text{—CH}_2\text{—I}$ [16, 20–30] 2-1 unit is about 25 times less reactive toward IDT than the isomeric $\text{P}_n\text{—CH}_2\text{—CF}_2\text{—I}$ 1,2-unit [28].

Once all the $\text{R}_\text{F—I}$ initiator is consumed via CT, no *new* PVDF–I chains are generated, and the only productive, thermodynamically neutral, uncatalyzed, *reversible* IDT, equilibrium ($K_{\text{equil(ex1)}} = 1$) between equally reactive, propagating and dormant $\text{P}_n\text{—CH}_2\text{—CF}_2\cdot$ and $\text{P}_m\text{—CH}_2\text{—CF}_2\text{—I}$ terminal 1,2-units (Equation 2.7), operates. Here, the exchange constant, $\text{C}_{\text{ex},1} = k_{1,\text{exchange}}^{\text{PVDF—CF}_2\cdot, \text{PVDF—CF}_2\text{—I}} / k_{\text{propagation, 1,2—addition}}^{\text{PVDF—CF}_2\cdot, \text{VDF}}$ is $\gg 1$ and thus exchange is favored over propagation and termination. However, due to the much stronger $\text{—CH}_2\text{—I}$ bond, the cross-IDT between the 1,2- and 2,1-units (Equation 2.8) is shifted toward the irreversible buildup of $\text{P}_n\text{—CF}_2\text{—CH}_2\text{—I}$ chain ends, whereas the IDT of the 2,1- terminal units is virtually inexistent (Equation 2.9) [27, 28].

Nonetheless, Equations 2.7ab, enable IDT–CRP, as demonstrated [51] (Figure 2.2) by the linear dependence of M_n on conversion and moderate PDI values, which indicate that $\text{Mn}_2(\text{CO})_{10}$ supports a photo-CRP over a wide range of molecular weights, and represents *the first example of metal-mediated VDF–CRP and the first example of visible light-mediated VDF–CRP*.

Mechanistically, however, with the exception of iodide chain end reactivation by $\text{Mn}(\text{CO})_5\cdot$ to compensate for termination, this remains a conventional IDT. Thus, while IDT catalysis would lead to PDI decrease [3, 9], control experiments [51] reveal that, consistent with PVAc-IDT [101, 102], the photochemically inactive [136a] $\text{Mn}(\text{CO})_5\text{—I}$ is incapable of donating I. Although $\text{R}_\text{F—Mn}(\text{CO})_5$ ($\text{R}_\text{F} = \text{CH}_2\text{F}$, CF_2H) [136b] derivatives exist, organometallic CRP mediation with $\text{PVDF—Mn}(\text{CO})_5$ via reversible C–Mn bond homolysis is discounted in view of the observed —I , not —H or $\text{—Mn}(\text{CO})_5$ chain ends, of the successful CRP with *catalytic*, not stoichiometric $\text{Mn}_2(\text{CO})_{10}$ vs. $\text{R}_\text{F—I}$, and of the relative order of the $\text{R}_\text{F—Mn}(\text{CO})_5$ (34) [74] $< (\text{CO})_5\text{Mn—Mn}(\text{CO})_5$ (38) [132b] $< \text{R}_\text{F—I}$ (48) [137] $< \text{I—Mn}(\text{CO})_5$ (54) [132] BDEs (kcal/mol), consistent with the photoinstability of Mn alkyls [132b].

2.3.3.2 Effect of Mono vs. Difunctional $\text{R}_\text{F—I}$ and $\text{I—R}_\text{F—I}$ Initiators $\text{I—R}_\text{F—I}$ initiators are particularly suitable for FM–CRPs, as bidirectional growth from difunctional propagating species [10], in conjunction with initiator or chain end halide activation by the continuously photogenerated $\text{Mn}(\text{CO})_5\cdot$ [138], (Equation 2.2) compensate for termination by radical coupling or transfer [10] and helps maintain a steady state radical concentration [51]. Indeed, termination is not as pronounced for the $\text{I—R}_\text{F—I}$ -initiated polymerizations, where dimerization of two propagating $\text{I—PVDF}\cdot$ radicals provides $\text{I—(PVDF)}_2\text{—I}$, or where H transfer affords I—PVDF—H . Thus, iodine chain end functionality is still retained, and can be reactivated by $\text{Mn}(\text{CO})_5\cdot$.

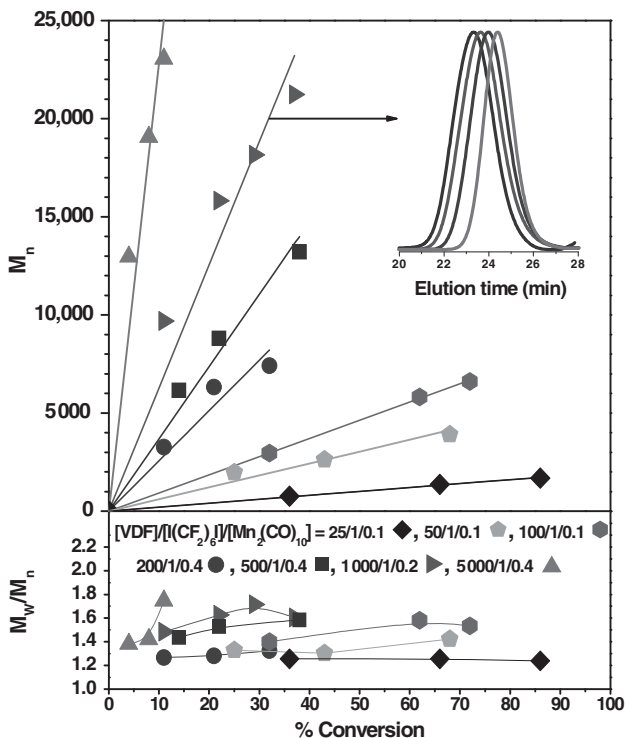


FIGURE 2.2 Dependence of M_n and M_w/M_n on conversion in $Mn_2(CO)_{10}$ -photomediated VDF-IDT-CRP. Reprinted with permission from Reference 51. Copyright 2012 American Chemical Society.

Indeed, even if two radicals are consumed, and one propagating chain end becomes endcapped as $-CF_2-CH_2-I$ or terminated by H transfer, the remaining $-CH_2-CF_2-I$ chain end may still get reversibly activated and propagate for some time and even undergo additional dimerizations. Thus, the probability of having $-CH_2-H$ or $-CF_2-H$ end groups is greatly reduced and the lifetime of the chains is increased. This dramatically improves the livingness of the polymerization, narrows the PDI values, and almost doubles the iodine chain end functionality.

2.3.3.3 Dependence of Halide Chain Ends and HH Units on Conversion As demonstrated by NMR, in IDT, HH defects ($\delta = 2.3\text{--}2.4$ ppm) are dramatically suppressed (Figure 2.1b.), being intercepted as $P_m-CF_2-CH_2-I$, and thus show no conversion dependence [51]. Obviously, IDT cannot control the regioselectivity of propagation, and the 2,1-addition is just *apparently* suppressed via CT to R_F-I . In reality, as $\sim PVDF-CF_2-CH_2\cdot$ is more reactive than $\sim PVDF-CH_2-CF_2\cdot$ ($k_{p,21} > k_{p,12}$), the diminishing of HH or of the terminal $-CH_2-H$ and $-CF_2-H$ units, is due to the faster CT to the reactive R_F-I initiators by comparison to propagation

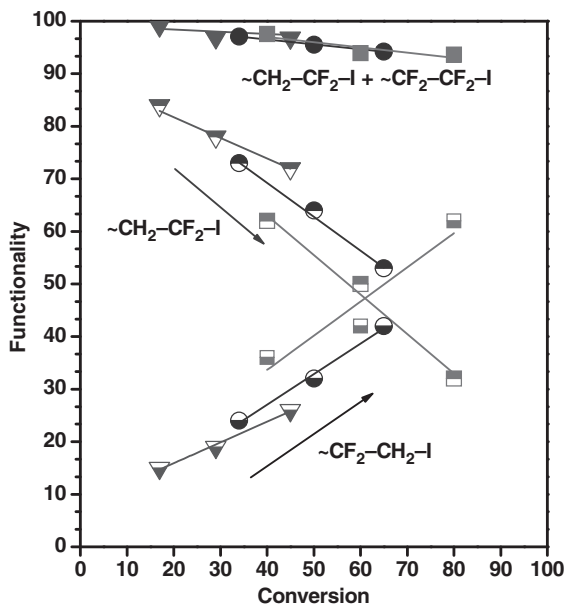


FIGURE 2.3 Dependence of the iodide chain end functionality on conversion in the $\text{Mn}_2(\text{CO})_{10}$ -mediated VDF-IDT-CRP. $[\text{VDF}]/[\text{I}(\text{CF}_2)_6\text{I}]/[\text{Mn}_2(\text{CO})_{10}] = 50/1/0.1$ (\blacktriangledown), $50/1/0.2$ (\bullet), $50/1/0.4$ (\blacksquare). Filled symbols = total functionality, top filled = $\sim\text{CH}_2\text{-CF}_2\text{-I}$, bottom filled = $\sim\text{CF}_2\text{-CH}_2\text{-I}$. Reprinted with permission from Reference 51. Copyright 2012 American Chemical Society.

($\text{CT}_{\text{RX}}^{\text{PVDF-CH}_2^*} > \text{CT}_{\text{RX}}^{\text{PVDF-CF}_2^*} > 1$), dimerization or H abstraction. Accordingly, once the 2,1-propagating unit is intercepted by the I of $\text{R}_\text{F}\text{-I}$, it is no longer able to propagate, transfer, or terminate, and instead, the potential HH unit is observed as the inactive $\text{PVDF-CF}_2\text{-CH}_2\text{-I}$. Nonetheless, its eventual reactivation if using excess $\text{Mn}(\text{CO})_5^*$, or much slower by IDT with $\sim\text{PVDF-CF}_2\text{-CH}_2^*$, could still provide an HH unit.

Since the $\text{PVDF-CH}_2\text{-I}$ termini are much less reactive, and thus not involved in IDT, they will accumulate (Figure 2.3) and will belong to a lower molecular weight population than the corresponding *dormant* $\text{PVDF-CF}_2\text{-I}$, which can still propagate. Similarly to VAc-IDT [101, 139], their accumulation will broaden the PDI, while their reactivation will require stronger halide abstractors than for the 1,2- $\text{PVDF-CF}_2\text{-I}$ unit [51]. Unfortunately, this also implies that the activator forms an even stronger bond with the halide. Indeed, while such reversible IDT *catalysis* with $\text{Mn}(\text{CO})_5\text{-I}$ would have prevented accumulation of $\text{P}_n\text{-CF}_2\text{-CH}_2\text{-I}$, this was not the case. As such, the $\text{P}_n\text{-CF}_2\text{-CH}_2\text{-I}$ chain ends are pretty much unresponsive as far as conventional, free radical initiated IDT or other metal mediated or organic chain end derivatizations are concerned [27]. Moreover, their concentration increases continuously with conversion, leaving a very bleak prospect for block

copolymerizations. Nonetheless, as explained above, the *total* ($-\text{CF}_2-\text{CH}_2-\text{I} + -\text{CF}_2-\text{CH}_2-\text{I}$) iodine functionality remains >95% in the case of difunctional initiators. This is a reasonable value, on condition that *both* chain ends can be reactivated, as is the case with stoichiometric $\text{Mn}(\text{CO})_5^\bullet$, below.

2.4 SYNTHESIS OF WELL-DEFINED BLOCK COPOLYMERS FROM PVDF-I AND I-PVDF-I CHAIN ENDS

Earlier tryouts at the synthesis of pseudo PVDF blocks included either attempting VDF initiation from macromolecular $\text{R}_\text{F}-\text{I}$ in the presence of free radical initiators [31, 140, 141] (which inherently produces PVDF homopolymer), or *assuming* that the chain ends of PVDF-X [141–144] were reactive enough to permit the radical initiation of another monomer (Cu/ATRP [142–144] or thermal IDT [141]), or polycondensations with polysulfone *bis*-nucleophiles [143]. Moreover, the dependence of the chain end functionality on conversion was never studied and acknowledged. Thus, with one exception [141], no details on the PVDF-X halide chain ends were provided, or the fact that mixtures are actually produced, was recognized and understood. In reality, CuX/L hardly activates perfluoroalkylhalides ($k_{\text{abstr}}^{(\text{CH}_3)_2\text{C}(\text{COOEt})-\text{Br}}/k_{\text{abstr}}^{\text{C}_8\text{F}_{17}-\text{Br}} \sim 10^2$) [145], and thus, would barely initiate from $-\text{CF}_2\text{CF}_2-\text{I}$, let alone from $-\text{CH}_2\text{CF}_2-\text{I}$, and especially from the unreactive $-\text{CF}_2-\text{CH}_2-\text{I}$ chain end. Similarly, radical ethyleneation [36, 146, 147] or azidation [148] are again available only for the $-\text{CH}_2-\text{CF}_2-\text{I}$ chain end, and only at high temperature (150–200°C) or under microwave irradiation. Finally, F strongly deactivates nucleophilic substitutions [36].

In retrospect, due to the failure of the respective chemistries to activate the stronger and dominant $-\text{CF}_2-\text{CH}_2-\text{X}$ termini, (as such experiments used high conversion PVDF-I samples, thus containing >80% of the inactive PVDF- CH_2-I), it is clear that all previous endeavors were futile and fundamentally incomplete, and that all so-called “blocks” were in fact *always* inseparable, ill-defined mixtures of PVDF- CH_2-I with PVDF-block copolymers [31, 140–144]. Likewise, as the dead PVDF- CH_2-I termini accumulate, they are always of *lower* molecular weight than the dormant/propagating PVDF- CF_2-I chain ends. Conceivably, selective precipitation/fractionation may enable enrichment in the PVDF- CF_2-I chain end [28], but this would be inefficient and difficult. Thus, the clean synthesis of “pure,” well-defined PVDF-block copolymers requires *complete* activation and/or derivatization of both types of PVDF chain ends, and especially of $\sim\text{CF}_2\text{CH}_2-\text{X}$.

As such, while the concentration of active $-\text{CH}_2-\text{CF}_2-\text{I}$ decreases and that of unreactive $-\text{CF}_2-\text{CH}_2-\text{I}$ increases with conversion, (Figure 2.3) [51], the *total* ($-\text{CH}_2-\text{CF}_2-\text{I} + -\text{CF}_2-\text{CH}_2-\text{I}$) iodine functionality remains at least 95%, even at larger levels of $\text{Mn}_2(\text{CO})_{10}$ [51]. This is adequate for block copolymer synthesis, if *both* halide chain ends can be activated, and this is where the high $\text{Mn}(\text{CO})_5^\bullet$ halide affinity [59] comes into play. Indeed, as seen above, $\text{Mn}(\text{CO})_5^\bullet$ was able to activate not only the $\sim\text{CF}_2-\text{I}$ based initiators, but even the CH_3-I , $\text{CH}_3-(\text{CH}_2)_5-\text{I}$, as well as $\text{H}-\text{CF}_2-\text{CF}_2-\text{CH}_2-\text{I}$ models of the reverse PVDF- $\text{CF}_2-\text{CH}_2-\text{I}$ 2,1-chain end

addition. Initiation from these inactivated, primary alkyl iodides is a remarkable result and indicates that $\text{Mn}_2(\text{CO})_{10}$ can easily activate even strong C–I bonds. Yet, the progressively more reactive $\sim\text{CF}_2\text{--CH}_2\text{--I}$ and $\sim\text{CH}_2\text{--CF}_2\text{--I}$ PVDF iodine chain are even easier to activate than regular alkyl iodides. As such, $\text{Mn}(\text{CO})_5^\bullet$ affords the clean and *quantitative* activation of *both* $\text{--CH}_2\text{--CF}_2\text{--I}$ and $\text{--CF}_2\text{--CH}_2\text{--I}$ chain ends. As such, regardless of polymerization conversion and thus their ratio in PVDF–I, they *both* represent viable substrates for the $\text{Mn}(\text{CO})_5^\bullet$ -based initiation, and enable the synthesis of well-defined PVDF-block copolymers with any radically polymerizable vinyl monomer. Therefore, $\text{Mn}_2(\text{CO})_{10}$ not only mediates IDT, but more importantly, and by contrast to other metal systems (e.g., Cu–ATRP), activates all chain ends for the initiation of a block copolymerization.

Selected examples of the ^1H -NMR characterization of such PVDF blocks are presented in Figure 2.4 [51]. Besides acetone and water ($\delta = 2.05$ and 2.84 ppm), the HT $\text{--CF}_2\text{--[CH}_2\text{--CF}_2\text{]}_n\text{--CH}_2\text{--}$, (a), and HH, $\text{--CF}_2\text{--CH}_2\text{--CH}_2\text{--CF}_2\text{--}$ (a') PVDF linkages [36, 149] are seen at $\delta = 2.8\text{--}3.1$ ppm and $\delta = 2.3\text{--}2.4$ ppm. Resonance **b** ($\delta = 3.25$ ppm) confirms the $\text{R}_\text{F}\text{--CH}_2\text{--CF}_2\text{--}$ connectivity with the first polymer unit, while the 1,2- $\text{CH}_2\text{--CF}_2\text{--I}$ (c) and 2,1- $\text{CF}_2\text{--CH}_2\text{--I}$ (c'), iodine chain ends are

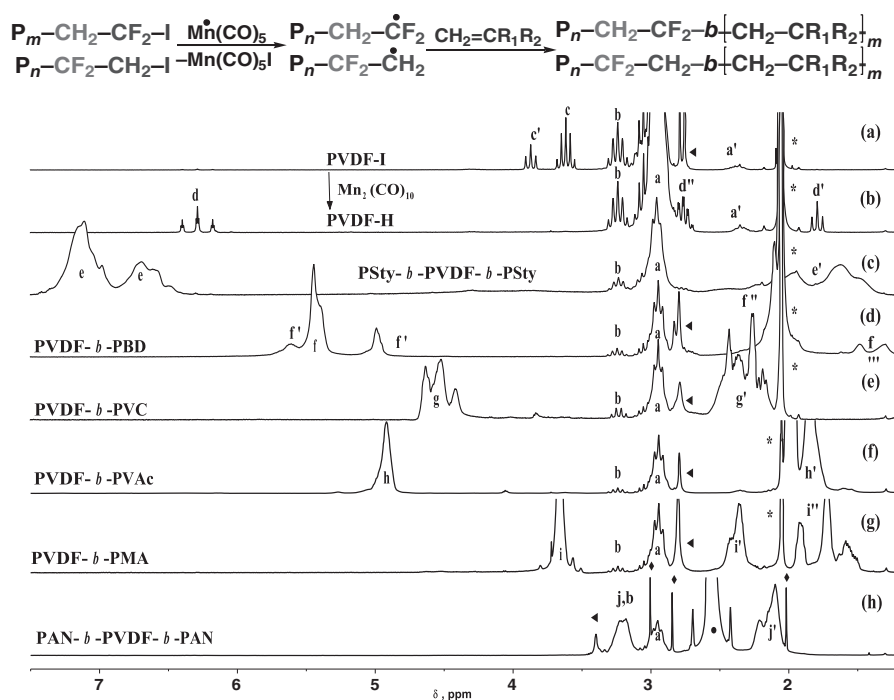


FIGURE 2.4 500 MHz ^1H -NMR spectra of PVDF–I, PVDF–H, and various PVDF-block copolymers. All in d_6 -acetone except PAN in d_6 -DMSO. \blacktriangleleft = H_2O , * = acetone, \blacklozenge = DMAC, \bullet = DMSO. Reprinted with permission from Reference 51. Copyright 2012 American Chemical Society.

seen [27] at $\delta = 3.62$ ppm and $\delta = 3.87$ ppm. Trace termination by H transfer to PVDF \cdot (Equations 2.11 and 2.12), (i.e., $-\text{CH}_2-\text{CF}_2-\text{H}$ and $-\text{CF}_2-\text{CH}_3$, peaks **d**, **d'**) is seen at $\delta = 6.30$ ppm and $\delta = 1.80$ ppm [149].

Upon treatment of PVDF-I with stoichiometric $\text{Mn}(\text{CO})_5\cdot$, as demonstrated by the disappearance of the **c** and **c'** peaks, *complete* radical activation of *both* iodide chain ends occurs, and the resulting PVDF \cdot radicals are deactivated by H abstraction from solvent, to afford the corresponding PVDF-H chain ends, seen as a dramatic increase in the **d** and **d'** peaks, and a more resolved $-\text{CH}_2-\text{CF}_2-\text{CH}_2-\text{CF}_2-\text{H}$ **d''**, $\delta = 2.77$ ppm [51, 149].

Thus, performing the activation in the presence of radically polymerizable alkenes leads to the first examples of well-defined AB or ABA-type PVDF-block copolymers with styrene (**e**, **e'**), butadiene (**f**, **f'**, **f''**, **f'''**), vinyl chloride (**g**, **g'**), vinyl acetate (**h**, **h'**), methyl acrylate (**i**, **i'**, **i''**), and acrylonitrile (**j**, **j'**), initiated from *both* the PVDF halide chain ends. While here $\text{Mn}_2(\text{CO})_{10}$ simply performs irreversible halide activation, and there is no IDT, control of the block copolymerization can be envisioned by other CRP methods.

2.5 CONCLUSIONS

We have demonstrated for the first time, that metal-catalyzed initiation of the polymerization of main chain fluorinated gaseous monomers such as VDF, can easily be accomplished at 0–100°C, including at rt upto 40°C, *directly* from a wide variety of alkyl, semifluorinated and perfluoroalkyl halides (Cl, Br, I), using a visible light, $\text{Mn}_2(\text{CO})_{10}$ photomediated protocol, carried out in low pressure glass tubes, and which is especially successful in dimethyl carbonate.

The use of perfluorinated alkyl iodides, particularly the difunctional $\text{I}-\text{R}_\text{F}-\text{I}$, enables the IDT mechanism, leading to CRPs, with very high (>95%) total iodide chain end functionality and <1% HH defects.

While the concentration of the active $-\text{CH}_2-\text{CF}_2-\text{I}$ decreases and that of unreactive $-\text{CF}_2-\text{CH}_2-\text{I}$ PVDF chain ends increases with conversion, their subsequent quantitative activation with $\text{Mn}_2(\text{CO})_{10}$ affords the first examples of well-defined PVDF-block copolymers with a variety of other classes of monomers, irrespective of the $-\text{CH}_2-\text{CF}_2-\text{I}/-\text{CF}_2-\text{CH}_2-\text{I}$ ratio in the PVDF-I sample.

The direct halide VDF initiation, VDF-IDT-CRP, and the quantitative iodide chain ends activation open up previously unavailable strategies for the photomediated synthesis of pure and well-defined, architecturally complex fluoromaterials. As such, main chain fluorinated monomers can be block copolymerized or grafted directly from any substrates featuring suitable halide initiators, while on the other hand, the polymerization of other monomers can be quantitatively initiated from the halide chain ends of such fluoropolymers, without the formation of mixtures. With multifunctional initiators, star and hyperbranched fluoropolymers can also be envisioned. Lastly, the $\text{R}_\text{F}-\text{I}/\text{Mn}_2(\text{CO})_{10}$ protocol is also applicable in radical trifluoromethylation and perfluoroalkylation reactions which are in great demand in organic chemistry [52].

REFERENCES

1. Ameduri, B. *Macromolecules* **2010**, *43*, 10163–10184.
2. Lena, F.; Matyjaszewski, K. *Prog. Polym. Sci.* **2010**, *35*, 959–1021.
3. Matyjaszewski, K.; Davis, T. P. *Handbook of Radical Polymerization*; John Wiley & Sons: New York, 2002.
4. Braunecker, W. A.; Matyjaszewski, K. *Prog. Polym. Sci.* **2007**, *32*, 93–146.
5. Goto, A.; Fukuda, T. *Progr. Polym. Sci.* **2004**, *29*, 329.
6. Fukuda, T. *J. Polym. Sci.: Part A: Polym. Chem.* **2004**, *42*, 4743–4755.
7. Ameduri, B. *Chem. Rev.* **2009**, *109*, 6632–6686.
8. Hansen, N. M. L.; Jankova, K.; Hvilsted, S. *Eur. Polym. J.* **2007**, *43*, 255–293.
9. Fukuda, T.; Goto, A.; Tsujii, Y. Kinetics of Living Radical Polymerization. In *Handbook of Radical Polymerization*; Matyjaszewski, K., Davis, T. P., Eds.; John Wiley & Sons: New York, 2002; pp 407–462.
10. Oka, M.; Tatemoto, M. Vinylidene Fluoride-Hexafluoropropylene Copolymer Having Terminal Iodines. In *Contemporary Topics in Polymer Science*; Bailey, W. J., Tsuruta, T., Eds.; Plenum Press: New York, 1984; Vol. 4, pp 763–781.
11. Tatemoto, M. *Int. Poly. Sc. Tech.* **1985**, *12*, 85–98.
12. Tatemoto, M. In *Polymeric Materials Encyclopedia*; Salamone, J. C., Ed.; CRC: Boca Raton, FL, 1996; Vol. 5, pp 3847–3862.
13. Tatemoto, M.; Shimizu, T. Thermoplastic Elastomers. In *Modern Fluoropolymers*; Scheirs, J., Ed.; John Wiley & Sons: New York, 1997; pp 565–576.
14. Tatemoto, M.; Nakagawa, T. US Patent 4,158,678, 1979.
15. Gaynor, S. G.; Wang, J. S.; Matyjaszewski, K. *Macromolecules* **1995**, *28*, 8051–8056.
16. David, G.; Boyer, C.; Tonnar, J.; Ameduri, B.; Lacroix-Desmazes, P.; Boutevin, B. *Chem. Rev.* **2006**, *106*, 3936–3962.
17. Boutevin, B. *J. Polym. Sci.: Part A: Polym. Chem.* **2000**, *38*, 3235–3243.
18. Ameduri, B.; Boutevin, B. *Top. Curr. Chem.* **1997**, *192*, 165–233.
19. Ameduri, B.; Boutevin, B. *Well Architected Fluoropolymers: Synthesis, Properties and Applications*; Elsevier: Amsterdam, 2004; pp 1–99.
20. Ameduri, B.; Ladavière, C.; Delolme, F.; Boutevin, B. *Macromolecules* **2004**, *37*, 7602–7612.
21. Montefusco, F.; Bongiovanni, R.; Priola, A.; Ameduri, B. *Macromolecules* **2004**, *37*, 9804–9813.
22. Cape, J. N.; Greig, A. C.; Tedder, J. M.; Walton, J. C. *J. Chem. Soc., Faraday Trans. 1: Phys. Chem. Condens. Phases* **1975**, *71*, 592.
23. Hauptschein, M.; Braid, M.; Lawlor, F. E. *J. Am. Chem. Soc.* **1958**, *80*, 846–851.
24. Soueni, A. E.; Tedder, J. M.; Walton, J. C. *J. Fluor. Chem.* **1978**, *11*, 407–417.
25. Combes, J. R.; Guan, Z.; DeSimone, J. M. *Macromolecules* **1994**, *27*, 865–886.
26. Balague, J.; Ameduri, B.; Boutevin, B.; Caporiccio, G. *J. Fluorine Chem.* **1995**, *70*, 215–223.
27. Boyer, C.; Valade, D.; Sauguet, L.; Ameduri, B.; Boutevin, B. *Macromolecules* **2005**, *38*, 10353–10362.

28. Boyer, C.; David, V.; Lacroix-Desmazes, P.; Ameduri, B.; Boutevin, B. *J. Polym. Sci.: Part A: Polym. Chem.* **2006**, *44*, 5763–5777.
29. Imran-ul-haq, M.; Förster, N.; Vukicevic, R.; Herrmann, K.; Siegmann, R.; Beuermann, S. *ACS Symp. Ser.* **2009**, *1024*, 233–243.
30. Apostolo, M.; Arcella, V.; Storti, G.; Morbidelli, M. *Macromolecules* **2002**, *35*, 6154–6166.
31. Valade, D.; Boyer, C.; Ameduri, B.; Boutevin, B. *Macromolecules* **2006**, *39*, 8639–8651.
32. MacMurray, N.; Tedder, J. M.; Vertommen, L. L. T.; Walton, J. C. *J. Chem. Soc., Perkin Trans.* **1976**, *2*, 63–69.
33. Hung, M. H. US Patent 5,231,154, 1993.
34. Low, H. C.; Tedder, J. M.; Walton, J. C. *J. Chem. Soc., Faraday Trans. 1: Phys. Chem. Condens. Phases* **1976**, *72*, 1707.
35. Apostolo, M.; Arcella, V.; Storti, G.; Morbidelli, M. *Macromolecules* **1999**, *32*, 989.
36. Ameduri, B.; Boutevin, B. *J. Fluorine Chem.* **1999**, *100*, 97–116.
37. Zhang, Z. C.; Chung, T. C. *Macromolecules* **2006**, *39*, 5187–5189.
38. Balague, J.; Ameduri, B.; Boutevin, B.; Caporiccio, G. *J. Fluorine Chem.* **2000**, *102*, 253–268.
39. Nguyen, B. V.; Yang, Z. Y.; Burton, D. J. *J. Org. Chem.* **1998**, *63*, 2887–2891.
40. Li, A. R.; Chen, Q. Y. *J. Fluorine Chem.* **1997**, *81*(2), 99–101.
41. Chen, M. Y.; Yang, Z. Y.; Zhao, C. X.; Qiu, Z. M. *J. Chem. Soc. Perkin Trans. I.* **1988**, *3*, 563.
42. Metzger, J. O.; Linker, U. *Liebigs Ann. Chem.* **1992**, *3*, 209–216.
43. Hu, C. M.; Qiu, Y. L. *J. Chem. Soc. Perkin Trans. I.* **1992**, *13*, 1569–1572.
44. Huang, W. Y.; Zhang, H. Z.; Lu, L. *J. Fluorine Chem.* **1990**, *50*(1), 133–140.
45. Leung, L.; Linclau, B. *J. Fluorine Chem.* **2008**, *129*, 986–990.
46. Fang, X.; Yang, X.; Yang, X.; Mao, S.; Wang, Z.; Chena, G.; Wua, F. *Tetrahedron.* **2007**, *63*, 10684–10692.
47. Hu, C. M.; Qing, F. L. *J. Org. Chem.* **1991**, *56*, 6348–6351.
48. Yang, Z. Y.; Burton, D. J. *J. Org. Chem.* **1991**, *56*, 1037–1041.
49. Tsunoi, S.; Ryu, I.; Fukushima, H.; Tanaka, M.; Komatsu, M.; Noburu, S. *Synlett.* **1999**, *5*, 1249–1252.
50. Benefice-Malouet, S.; Blancou, H.; Commeyras, A. *J. Fluorine Chem.* **1993**, *63*(3), 217–226.
51. Asandei, A. D.; Adebolu, O. I.; Simpson, C. P. *J. Am. Chem. Soc.* **2012**, *134*, 6080–6083.
52. Asandei, A. D.; Adebolu, O. I.; Simpson, C. P.; Kim, J. S. *Angew. Chem. Int. Ed.* **2013**, *52*, 10027–10030.
53. Asandei, A. D.; Simpson, C. P.; Adebolu, O.; Chen, Y. *Polym. Prepr.* **2011**, *52*(2), 728–729.
54. Asandei, A. D.; Adebolu, O. I.; Simpson, C. P. *Acs. Symp. Ser.* **2012**, *1106*, 47–63.
55. Asandei, A. D.; Simpson, C. P.; Adebolu, O.; Chen, Y. *Polym. Prepr.* **2011**, *52*(2), 554–555.
56. Sauguet, L.; Boyer, C.; Ameduri, B.; Boutevin, B. *Macromolecules* **2006**, *39*, 9087–9101.
57. Messina, M. T.; Metrangolo, P.; Resnati, G. *ACS Symp. Ser.* **1999**, *746*, 239–254.

58. Rowlands, G. J. *Tetrahedron* **2009**, 65, 8603–8655.
59. Gilbert, B. C.; Parsons, A. F. *J. Chem. Soc., Perkin Trans. 2*. **2002**, 3, 367–387.
60. Haszeldine, R. N.; Steele, B. R. *J. Chem. Soc.* **1954**, 923.
61. Saint-Loup, R.; Ameduri, B. *J. Fluorine Chem.* **2002**, 116, 27–34.
62. Asandei, A. D.; Chen, Y. *Polym. Mater: Sci. Eng.* **2008**, 98, 346–347.
63. Asandei, A. D.; Chen, Y. *Polym. Prepr.* **2007**, 48(2), 452–453.
64. Asandei, A. D.; Chen, Y. *Polym. Mater: Sci. Eng.* **2007**, 97, 270–271.
65. Asandei, A. D.; Chen, Y. *Polym. Prepr.* **2005**, 46(2), 633.
66. Asandei, A. D.; Moran, I. W. *J. Am. Chem. Soc.* **2004**, 126, 15932–15933.
67. Asandei, A. D.; Simpson, C. P.; Yu, H. S.; Adebolu, O. I.; Saha, G.; Chen, Y. *ACS Symp. Ser.* **2009**, 1024, 149–166.
68. Abrahamson, H. B.; Wrighton, M. S. *J. Am. Chem. Soc.* **1977**, 99, 5510–5512.
69. Meckstroth, W. K.; Walters, R. T.; Waltz, W. L.; Wojcicki, A.; Dorfman, L. M. *J. Am. Chem. Soc.* **1982**, 104, 1842–1846.
70. Fawcett, J. P.; Poe, A.; Sharma, K. R. *J. Chem. Soc., Dalton Trans.: Inorg. Chem.* **1979**, 12, 1886–1890.
71. Brimm, E. O.; Lynch, M. A., Jr.; Sesny, W. J. *J. Am. Chem. Soc.*, **1954**, 76(14), 3831–3835.
72. Treichel, P. M. Manganese carbonyls and manganese carbonyl halides. In *Comprehensive Organometallic Chemistry II Vol. 6, Manganese Group*; Abel, E. W., Stone, F. G. A., Wilkinson, G., Casey, C. P., Eds.; Pergamon, 1995; pp 1–19.
73. Tenhaeff, S. C.; Covert, K. J.; Castellani, M. P.; Grunkemeier, J.; Kunz, C.; Weakley, T. J. R.; Koenig, T.; Tyler, D. R. *Organometallics* 1993, 12, 5000–5004.
74. Martinho Simoes, J. A.; Beauchamp, J. A. *Chem. Rev.* **1990**, 90, 629–688.
75. Friestad, G. K.; Qin, J. *J. Am. Chem. Soc.* **2001**, 123, 9922–9923.
76. Jackson, R. A.; Poe, A. *Inorg. Chem.* **1978**, 17, 997–1003.
77. Fawcett, J. P.; Poe, A.; Sharma, K. R. *J. Am. Chem. Soc.* **1976**, 98, 1401.
78. Rothberg, L. J.; Cooper, J. N.; Peters, K. S.; Vaida, V. *J. Am. Chem. Soc.* **1982**, 104, 3536–3537.
79. (a) Robert, H. C.; Michael, P., Eds. *Comprehensive Organometallic Chemistry III, Volume 5*; Elsevier: Providence, RI, 2007; pp 440–746. (b) Zhang, J. Z.; Harris, C. B. *J. Chem. Phys.* **1991**, 95(6), 4024–4032.
80. Sarakha, M. Ferraudi, G. *Inorg. Chem.* **1999**, 38, 4605–4607.
81. Sullivan, R. J.; Brown, T. L. *J. Am. Chem. Soc.* **1991**, 113, 9155–9161.
82. Gilbert, B. C.; Kalz, W.; Lindsay, C. I.; McGrail, P. T.; Parsons, A. F.; Whittaker, D. T. E. *J. Chem. Soc., Perkin Trans. 1*. **2000**, 1187–1194.
83. Gilbert, B. C.; Lindsay, C. I.; McGrail, P. T.; Parsons, A. F.; Whittaker, D. T. E. *Synth. Commun.* **1999**, 29(15), 2711–2718.
84. Hallock, S. A.; Wojcicki, A. *J. Organomet. Chem.* **1979**, 182(4), 521–535.
85. Herrick, R. S.; Herrinton, T. R.; Walker, H. W.; Brown, T. L. *Organometallics* **1985**, 4, 42–45.
86. Bamford, C. H.; Mahmud, M. U. *J. Chem. Soc., Chem. Commun.* **1972**, 13, 762–763.
87. Bamford, C. H.; Mullik, S. U. *Polymer* **1973**, 14(1), 38–39.

88. Bamford, C. H.; Mullik, S. U. *Polymer* **1976**, 17(3), 225–230.
89. Aliwi, S. M.; Bamford, C. H.; Mullik, S. U. *J. Polym. Sci., Polym. Symp.* **1975**, 50, 33–50.
90. Bamford, C. H.; Mullik, S. U. *J. Chem. Soc., Faraday Trans. 1.* **1975**, 71(3), 625–636.
91. Bamford, C. H.; Mullik, S. U. *Polymer* **1976**, 17, 94–95.
92. Bamford, C. H.; Mullik, S. U. *J. Chem. Soc., Faraday Trans. 1.* **1976**, 72(2), 368–375.
93. Bamford, C. H.; Denyer, R. *Nature* **1968**, 217, 59–60.
94. Bamford, C. H.; Duncan, F. J.; Reynolds, R. J. W.; Seddon, J. D. *J. Polym. Sci., Part C: Polym. Symp.* **1968**, 23, 419–432.
95. Bamford, C. H.; Dyson, R. W.; Eastmond, G. C. *J. Polym. Sci., Part C.* **1967**, 16, 2425.
96. Jiang, M.; Wang, S.; Jin X. *J. Mater. Sci. Lett.* **1990**, 9, 1239–1240.
97. Jenkins, D. W.; Hudson, S. M. *Macromolecules* **2002**, 35, 3413.
98. Eastmond, G. C.; Parr, K. J.; Woot, J. *Polymer* **1988**, 29(5), 950–957.
99. Eastmond, G. C.; Richardson, J. E. *Macromolecules* **1991**, 24, 3189–3200.
100. Iskin, B.; Yilmaz, G.; Yagci, Y. *Macromol. Chem. Phys.* **2013**, 214, 94–98.
101. Koumura, K.; Satoh, K.; Kamigaito, M. *Macromolecules* **2008**, 41(20), 7359–7367.
102. Koumura, K.; Satoh, K.; Kamigaito, M. *J. Polym. Sci.: Part A: Polym. Chem.* **2009**, 47, 1343–1353.
103. Koumura, K.; Satoh, K.; Kamigaito, M. *Macromolecules* **2009**, 42, 2497–2504.
104. Kimura, K.; Satoh, K.; Kamigaito, M. *Polym. J.* **2009**, 41, 595–603.
105. Doll, W. W.; Lando, J. B. *J. Appl. Polym. Sci.* **1970**, 14(7), 1767–1773.
106. Russo, S.; Behari, K.; Chengji, S.; Pianca, M.; Barchiesi, E.; Moggi, G. *Polymer* **1993**, 34(22), 4777–4781.
107. Duc, M.; Ameduri, B.; Boutevin, B.; Kharroubi, M.; Sage, J.-M. *Macromol. Chem. Phys.* **1998**, 199, 1271–1289.
108. Galin, M.; Maslinkot, L. *Macromolecules* **1985**, 18, 2192–2196.
109. Galin, J. C.; Luttringer, G.; Galin, M. *J. Appl. Polym. Sci.* **1989**, 37, 487–498.
110. Luttringer, G.; Meurer, B.; Weill, G. *Polymer* **1991**, 32, 884–891.
111. Kuttringer, G.; Weill, G. *Polymer* **1991**, 32, 877–883.
112. Bottino, A.; Campanelli, G.; Munari, S.; Turturro, A. *J. Polym. Sci.: Part B: Polym. Phys.* **1988**, 26, 785–794.
113. Lee, W. H. Cyclic Carbonates. In *Chemistry of Nonaqueous Solvents Vol. 4*; Lagowski, J. J., Ed.; Academic Press: New York, 1976; p 167.
114. Odian G. *Principles of Polymerization*, 4th ed.; John Wiley & Sons, 2004; pp 292–298.
115. Ahmeda, T. S.; DeSimone, J. M.; Roberts, G. W. *Chem. Eng. Sci.* **2010**, 65, 651–659.
116. DiNoia, T. P.; Conway, S. E.; Lim, J. S.; Mchugh, M. A. *J. Polym. Sci., Part B: Polym. Phys.* **2000**, 38, 2832–2840.
117. Tundo, P.; Selva, M. *Acc. Chem. Res.* **2002**, 35, 706–716.
118. Gordon, A. S.; Norris, W. P. *J. Phys. Chem.* **1965**, 69(9), 3013–3017.
119. Thynne, J. C. J.; Gray, P. *Trans. Faraday Soc.* **1962**, 58, 2403–2409.
120. Wijnen, M. H. J. *J. Chem. Phys.* **1961**, 34, 1465–1466.
121. Yee Quee, M. J.; Thynne, J. C. J. *Trans. Faraday Soc.* **1966**, 62, 3154–3161.
122. Zeldes, H.; Livingston, R. *J. Magn. Reson.* **1976**, 21(1), 109–113.

123. Bilde, M.; Møgelberg, T. E.; Sehested, J.; Nielsen, O. J.; Wallington, T. J.; Hurley, M. D.; Japar, S. M.; Dill M., Orkin, V. L.; Buckley, T. J.; Huie, R. E.; Kurylo, M. J. *J. Phys. Chem. A* **1997**, *101*, 3514–3525.
124. Griller D.; Roberts, B. P. *J. Chem. Soc. Perkin Trans. II* **1972**, *6*, 747–751.
125. McRae, J. A.; Symons, M. C. R. *J. Chem. Soc. (B), Phys. Org.* **1968**, 428–430.
126. Hudson, R. L.; Williams, F. J. *Phys. Chem.* **1981**, *85*(5), 510–511.
127. Freunberger, S. A.; Chen, Y.; Peng, Z.; Griffin, J. M.; Hardwick, L. J.; Barde, F.; Novak, P.; Bruce, P. G. *J. Am. Chem. Soc.* **2011**, *133*, 8040–8047.
128. Burchill, M. T. Diffusion Effects of Carbonate Solvents in PVDF and PVDF Copolymers. In *Progress in Batteries and Battery Materials*; 1998, Vol. 17, pp 144–156, ITE-JEC Press.
129. Saunier, J.; Alloin, F.; Sanchez, J. Y.; Barriere, B. *J. Polym. Sci.: Part B: Polym. Phys.* **2004**, *42*, 532–543.
130. Saunier, J.; Alloin, F.; Sanchez, J. Y.; Barriere, B. *J. Polym. Sci.: Part B: Polym. Phys.* **2004**, *42*, 544–552.
131. Saunier, J.; Alloin, F.; Sanchez, J. Y.; Maniguet, L. *J. Polym. Sci.: Part B: Polym. Phys.* **2004**, *42*, 2308–2317.
132. (a) Drago, R. S.; Wong, N. M.; Ferris, D. C. *J. Am. Chem. Soc.* **1992**, *114*, 91–98.
(b) Friestad, G. K.; Marie, J. C.; Suh, Y. S.; Qin, J. J. *Org. Chem.* **2006**, *71*, 7016.
133. Duc, M.; Ameduri, B.; Ghislain, D.; Boutevin, B. *J. Fluorine Chem.* **2007**, *128*, 144–149.
134. Hallock, S. A.; Wojcicki, A. *J. Organomet. Chem.* **1979**, *182*, 521–535.
135. Dolbier, W. R., Jr. *Top. Curr. Chem.* **1997**, *192*, 97–163.
136. (a) Pan, X.; Philbin, C. E.; Castellani, M. P.; Tyler, D. R. *Inorg. Chem.* **1988**, *27*, 671–676.
(b) Martinho Simoes, J. A.; Beauchamp, J. L. *Chem. Rev.* **1990**, *90*, 629–688.
137. Okafo, E. N.; Whittle, E. *Int. J. Chem. Kinet.* **1975**, *7*, 287–300.
138. Sarakha, M.; Ferraudi, G. *Inorg. Chem.* **1999**, *38*, 4605.
139. Koumura, K.; Satoh, K.; Kamigaito, M. *Macromolecules* **2006**, *39*, 4054–4061.
140. Gelin, M.; Ameduri, B. *J. Polym. Sci.: Part A. Polym. Chem.* **2003**, *41*, 160–171.
141. Laruelle, G.; Nicol, E.; Ameduri, B.; Tassin, J. F.; Ajellal, N. *J. Polym. Sci. Part A: Polym. Chem.* **2011**, *49*, 3960–3969.
142. Ming, E.; Tsang, W.; Shi, Z.; Holdcroft, S. *Macromolecules* **2011**, *44*, 8845–8857.
143. Yang, Y.; Shi, Z.; Holdcroft, S. *Macromolecules* **2004**, *37*, 1678–1681.
144. Jol, S. M.; Lee, W. S.; Ahn, B.S.; Park, K Y.; Kim, K. A.; Paeng, I. R. *Polym. Bull.* **2000**, *44*, 1–8.
145. Sauguet, L.; Boyer, C.; Ameduri, B.; Boutevin, B. *Macromolecules* **2006**, *39*, 9087–9101.
146. Manseri, A.; Ameduri, B.; Boutevin, B.; Kotora, M.; Caporiccio, G. *J. Fluorine Chem.* **1997**, *81*, 103–113.
147. Balague, J.; Ameduri, B.; Boutevin, B.; Caporiccio, G. *J. Fluorine Chem.* **2000**, *102*, 253–268.
148. Vukicevic, R.; Beuermann, S. *Macromolecules* **2011**, *44*, 2597–2603.
149. Wormald, P.; Ameduri, B.; Harris, R. K.; Hazendonk, P. *Polymer* **2008**, *49*, 3629–3638.